Approaches for Automatic GCP Extraction and Localization in Airborne SAR Images and Some Test Results

Associate Prof. Dr.-Ing. Jaan-Rong Tsay1
Department of Geomatics, National Cheng Kung University
No. 1, University Road, Tainan 701, Taiwan, R.O.C.
tsayjr@mail.ncku.edu.tw

M. Sc. Pang-Wei Liu2
Department of Geomatics, National Cheng Kung University
No. 1, University Road, Tainan 701, Taiwan, R.O.C.

Abstract: This paper presents simple feature-based approaches for full- and/or semi-automatic extraction, selection, and localization (center-determination) of ground control points (GCPs) for radargrammetry using airborne synthetic aperture radar (SAR) images. Test results using airborne NASA/JPL TOPSAR images in Taiwan verify that the registration accuracy is about 0.8~1.4 pixels. In c.a. 30 minutes, 1500~3000 GCPs are extracted and their point centers in a SAR image of about 512 x 512 pixels are determined on a personal computer.

Keywords: Image Registration, Ground Control Point (GCP).

1. Introduction

Manual image registration for measuring tie points and/or GCPs on synthetic aperture radar (SAR) images for a wide variety of radargrammetry applications could be well established, but the procedure can lead to inaccurate and unreliable results, and also can be very time-consuming to execute. The subject of automatic image registration addresses, and in many cases solves, the problem associated with manual image registration. However, there still exist a number of scenarios where automatic image registration is not well developed and robust paradigms have not been established for multi-source image registration and image to map registration [1]. It motivates [2] to incorporate multiple algorithms into an automatic image registration system for extracting different types of features (such as points, lines, and polygons) and thus to increase the number of tie points and the quality of the registration of the images. This paper tries to further utilize more high-level information (such as feature-related topological relationship) involved in images. The techniques for registering multi-source images based on feature matching have been well discussed in [3].

In this paper, the complexity of the above-mentioned problem is reduced by only considering the registration of ortho-rectified images based on different horizontal datum, since the only available NASA/JPL TOPSAR power images are already ground range projected ones generated by using InSAR-determined digital elevation models (DEMs). Under the circumstances, this paper introduces two simple approaches to semi- and full-automatic feature based image registration in order to solve the problem of registration of airborne SAR and aerial ortho imagery, where high resolution aerial images are used as master images, and airborne SAR images are slave ones.

2. Semi- and Full-Automatic Approaches

Both approaches contain the following operation steps:
Step 1 - *image scaling*: the image resolutions of different sources are often very different. For making later registration operations easy, finer images are convoluted with a Gaussian kernel in order to generate their coarser resolution versions. Thus, the pixel sizes of all images are approximately the same.
Step 2 – *initial registration*: only as few conjugate points as possible are measured manually in the semi-automatic approach, whereas the full-automatic approach needs only the known geo-referencing data [5] of TOPSAR images. The images are then approximately aligned using the manually selected tie points (or geo-referencing data) and a first order transformation, in order to remove large difference in scale and rotation. In our registration of a TOPSAR image with an aerial ortho image, a linear conformal transformation model (1) is used. After the transformation parameters are determined, the co-registered slave image (SAR image) is interpolated by using the parametric cubic convolution (PCC) proposed by [4], in order to minimize the reconstruction error and to decrease the number of interpolation operations.

$$\begin{bmatrix} c' \\ r' \end{bmatrix} = S \begin{bmatrix} \cos\theta & \sin\theta \\ -\sin\theta & \cos\theta \end{bmatrix} \begin{bmatrix} c \\ r \end{bmatrix} + \begin{bmatrix} \Delta c \\ \Delta r \end{bmatrix} \qquad (1)$$

Step 3 – *fine registration*: if necessary, the strategy of image pyramid with l levels will be applied, in order to provide better initial registration parameters. On each resolution level, line features on both master and slave images are extracted by using the Förstner operator [6]. Then, both end points and inflection points on each feature line are used as interest points. As shown in Fig. 1, a pixel on a feature line is selected as a new interest point, if its vertical distance to the straight line connecting two nearest interest points on its both sides is maximal and

larger than a given threshold. A template of $m \times m$ pixels is then centered at an interest point P' on master image. A candidate template of the same size is then moving on slave image in a searching window centered at the approximate conjugate point P" of P'. P" is determined by using the initial transformation parameters and the coordinates (c', r') of P'. For each candidate template, the overlap q is computed as follows:

$$q = \frac{n\_cover}{n\_total} \qquad (2)$$

where *n_cover* is the number of overlapped pixels on feature lines in both master and slave templates, *n_total* is the number of pixels on all feature lines in the master template. If *n_total* is less than a threshold *n*, the window is not adopted. Moreover, the orientation angle α of a local feature line passing through an interest point is computed in both master and slave images. All interest point pairs with a local maximum q-value in the searching window and the difference of the α-values at P' and P" less than a given threshold δ are used to determine a set of new transformation parameters by using the least squares adjustment. Those pairs with the residuals larger than $n\hat{\sigma}_0$ will be deleted from the set of interest point pairs.

Step 4 – *GCP data acquisition*: the horizontal coordinate of each interest point can be computed by transforming the image coordinates (c, r) in the aerial ortho image into the ground horizontal coordinate system. The corresponding vertical coordinate can be interpolated e.g. from digital topographic maps or reference DTMs.

3. Test Results

Fig. 2 shows the aerial ortho image and the NASA/JPL TOPSAR power image in the test area A in the Chiayi county in Taiwan, where (E,N) denotes the ground horizontal coordinates and (L,S) denotes the (line, sample)-coordinates of the TOPSAR image rectified with ground range projection. Since the TOPSAR images have much coarser groundel size (5m×5m) than the one (0.64m×0.64m) of aerial ortho image, aerial ortho images are convoluted to form their coarser version with a groundel size of 5.12m× 5.12m. As shown in Fig. 3, manual selection of GCPs on TOPSAR images will be inaccurate and time-consuming due to coarse resolution and SAR image noise. Besides, Fig. 3 also shows that area-based matching (such least squares image matching) would not be a suitable technique for registering aerial image with SAR image due to different image scenery and low correlation in the processed window.

The images are then approximately aligned using the manually selected three tie points as shown in Fig. 4 (or geo-referencing data) and the linear conformal transformation, in order to remove large difference in scale and rotation. Then, the Förstner operator is used to extract feature lines as shown in Fig. 5. Apparently, there exist much more short line segments on the TOPSAR image. Foe example, a template of 25×25 pixels is now used on each image pyramid level with l=4 for fine registration with n=2. The a posteriori standard deviation of unit weight is $\hat{\sigma}_0$=1.38 pixels and 1842 points are selected. Fig. 6 shows two example points with similar and different image textures, respectively. Different physical-radiometric responses of a ground object for optical and SAR-sensors form different image content. It generally causes inaccurate registration. Nevertheless, the proposed approach still can provide better registration results. Moreover, if the orientation condition of $d\alpha<45°$ is further applied, a better results with $\hat{\sigma}_0$=1.36 pixels and 1782 more reliable points are selected automatically.

Compared with the results determined by the semi-automatic approach (SAA), the full-automatic approach (FAA) provides better registration accuracy with $\hat{\sigma}_0$ = 0.80 pixels, as shown in Table 1.

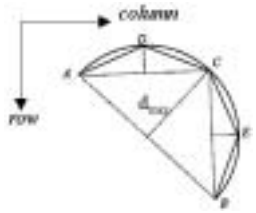

Fig. 1. Determining interest points on a feature line AB.

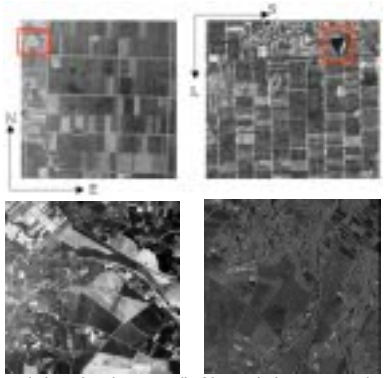

Fig. 2. The aerial ortho image (left) and the NASA/JPL TOPSAR power image (right) in the test area A of 493×493 pixels (bottom).

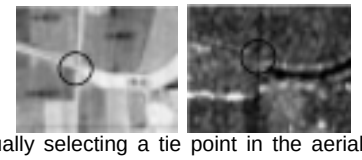

Fig. 3. Manually selecting a tie point in the aerial ortho image (left, 40×50 pixels) and TOPSAR image (right, 40×50 pixels) in the same area.

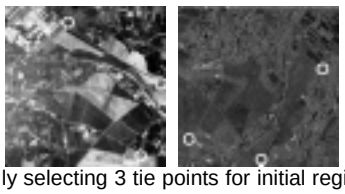

Fig. 4. Manually selecting 3 tie points for initial registration in the test area A of 2.5×2.5km.

Fig. 7 shows the images in another test areas B and C. The test area B of 493×493 pixels also covers a relatively flat farm field of 2.5×2.5km. The test area C of 512×512 pixels covers an area of 2.0×2.0km in the A-Li mountain region. The registration accuracy is 1.38 pixels and 1.40 pixels, respectively. The histogram of orientation angle differences dα of all feature lines on all matched interest points in three test areas is shown in Fig. 8. It clearly illustrates that many more matched points in the mountain area still have larger dα-values. However , the registration accuracy still can remain better due to the constrain on the searching window.

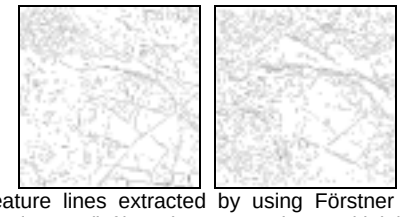

Fig. 5. Feature lines extracted by using Förstner operator in aerial ortho image (left) and TOPSAR image (right) in the test area A.

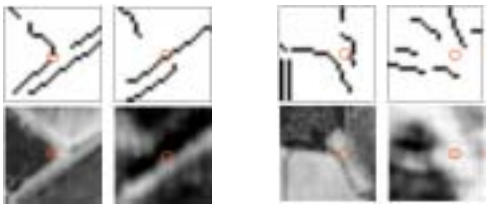

(1) q=0.57, *n_total*=29 (2) q=0.19, *n_total*=11

Fig. 6. Visual check of two matched interest points in a template of 25×25 pixels showing feature lines (top) and image window (bottom) for aerial ortho image (left) and TOPSAR image (right).

Table 1. Results of the SAA and FAA approaches in the test area A(*N*=number of matched points, $\hat{\sigma}_0$ = a posteriori standard deviation of unit weight, RMSD(c,r) = root mean square difference in the (column, row) coordinates.

method	*N*	$\hat{\sigma}_0$ (pixels)	RMSD(c,r) (pixels)	
SAA	1782	1.36	1.37	1.36
FAA	1795	0.80	0.82	0.79

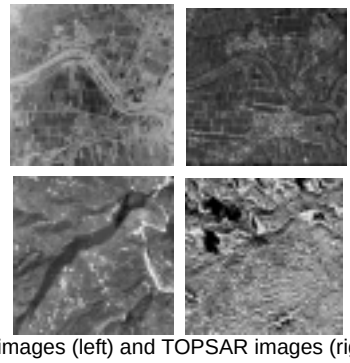

Fig. 7. Aerial images (left) and TOPSAR images (right) in the test area B (top) and test area C (bottom).

Table 2. Results of the FAA approach in the test areas B and C.

test area	*N*	$\hat{\sigma}_0$ (pixels)	RMSD(c,r) (pixels)	
B	3106	1.38	1.43	1.34
C	3292	1.40	1.42	1.38

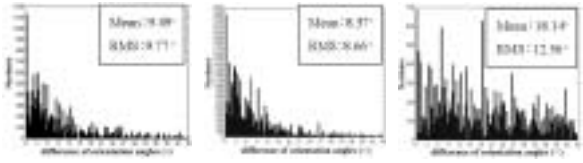

Fig. 8. Histogram of orientation angle differences dα of all feature lines on all matched interest points in the test area A (left), B (middle), and C (right).

4. Conclusions

This paper presents both SAA and FAA approaches for extracting, selecting and localizing ground control points for radargrammetry applications. The principle of image pyramid is utilized in the SAA approach in order to provide better initial values of registration parameters. All operations can be done automatically in the FAA approach. Both approaches utilize SAR image features and their topological relationship for efficiently and accurately registering aerial optical and SAR images. Test results show that a large number (c.a. 1500~3000) of GCPs across the entire image area can be determined in c.a. 30 minutes on a PC with a CPU speed of 1.4 GHz. The overall registration accuracy is 0.8~1.4 pixels.

Acknowledgement

We sincerely appreciate the National Science Council for supporting this work under the project numbers NSC90-2211-E-006-025, and NSC91-2211-E-006-112. TOPSAR data was collected on the PacRim 2000 Mission directed by the Center for Space and Remote Sensing Research (CSRSR) at National Central University and the Council of Agriculture at Executive Yuen, R.O.C..

References

[1] Dowman, I.J., and Dare, P.M., 1999. Automated Procedures for Multisensor Registration and Orthorectification of Satellite Images. *International Archives of Photogrammetry and Remote Sensing*, 32(7-4-3 W6): 37-44.

[2] Dare, P.M., and Dowman, I.J., 2001. An Improved Model for Automatic Feature-Based Registration of SAR and SPOT Images. *ISPRS Journal of Photogrammetry and Remote Sensing*, 56: 13-28.

[3] Fonseca, L., and Manjunath, B., 1996. Registration Techniques for Multisensor Remotely Sensed Imagery. *Photogrammetric Engineering and Remote Sensing*, 62(9): 1049-1056.

[4] Park, S.K., and Schowengerdt, R.A., 1983. Image Reconstruction by Parametric Cubic Convolution. *Computer Vision, Graphics and Image Processing*, 23: 258-272.

[5] **URL:** AIRSAR Integrated Processor Documentation (data formats), version 0.15, available on 13 May 2002 at http://airsar.jpl.nasa.gov/data/data_format.pdf.

[6] Förstner, W., 1993. Feature Extraction in Digital Photogrammetry, *Photogrammetry Record*, 14(82): 595-611.